Journal of ELECTRONIC MATERIALS, Vol. 47, No. 5, 2018
https://doi.org/10.1007/s11664-018-6091-2

Duration of Thermal Stability and Mechanical Properties of Mg_2Si/Cu Thermoelectric Joints

LANLAN CAI,[1] PENG LI,[1,3] PEI WANG,[1] QI LUO,[1] PENGCHENG ZHAI,[2] and QINGJIE ZHANG[2]

1.—School of Mechanical and Electronic Engineering, Wuhan University of Technology, Wuhan 430070, Hubei, China. 2.—State Key Laboratory of Advanced Technology for Materials Synthesis and Processing, Wuhan University of Technology, Wuhan 430070, Hubei, China. 3.—e-mail: lp1968@whut.edu.cn

Preparing an effective and long-term reliable contact between a thermoelectric (TE) element and its electrode is a key issue in integrating TE elements into practical devices. In this work, Cu electrodes were bonded to Mg_2Si by using the spark plasma sintering (SPS) technique. To investigate their thermal stability, Mg_2Si/Cu joints were annealed in vacuum at different temperatures (500°C, 550°C, and 580°C) for different durations (24 h, 48 h, and 72 h). Scanning electron microscopy (SEM) images illustrated that an intermediate layer with thickness of approximately 10 μm developed between Mg_2Si and Cu during the sintering process. Electron probe microanalysis (EPMA) indicated that Mg, Si, and Cu diffused into each other and formed a τ_3-phase at the interlayer. After annealing at 500°C for 72 h, the Mg_2Si/Cu joints still possessed good adhesion and showed no cracks; the thickness and the elemental fractions within the interlayer did not show an obvious difference due to the thermal treatment. The electrical contact resistance increased slightly while the shear strength of the Mg_2Si/Cu joints decreased with increasing aging time. However, when increasing the annealing temperature to 550°C, cracks developed along the boundary of the intermediate layer close to the Cu layer. Severer cracks were observed with higher aging temperature of 580°C. Therefore, it is evident that the Mg_2Si/Cu joints exhibited good thermal reliability with stable microstructure, relatively unchanged electrical contact, and sufficient bonding strength at operating temperatures below 500°C.

Key words: Mg_2Si-based thermoelectric materials, Cu electrode, thermoelectric joints, contact properties, thermal stability

INTRODUCTION

Thermoelectric (TE) technology enables direct conversion of thermal into electrical energy without use of moving components. It has attracted attention for decades due to its expected contribution to current energy issues.[1] The performance of TE devices mainly depends on development of TE materials. Magnesium silicide (Mg_2Si)-based TE materials have attracted keen interest due to their advantages of nontoxicity, light weight, low cost, and high natural abundance. They have been confirmed to exhibit high figure of merit of up to 1.5,[2–4] superior power factor of 5.18×10^{-3} W/m K^2,[5,6] and long-time stability[7,8] when operating in the intermediate temperature range from 600 K to 900 K. Therefore, Mg_2Si-based materials show promising prospects for use in TE generator applications. However, a key problem in developing TE materials into TE modules is creation of an effective and long-time stable contact between the TE element and its electrode.

A prerequisite for fabrication of a good TE junction is selection of an appropriate electrode material. It is

(Received July 28, 2017; accepted January 13, 2018; published online February 2, 2018)

well known that good electrode materials should have high electrical and thermal conductivity, as well as coefficient of thermal expansion (CTE) similar to those of TE materials. Previous studies have indicated that Ni and Cu are commonly used electrode materials; For example, Ni foil was successfully connected to *n*-type PbTe, but reaction and diffusion between Ni and PbTe will continue during device operation.[9] To hinder such diffusion, different buffer and barrier materials inserted between Ni electrodes and skutterudite materials have been studied.[10,11] Cu electrode was reported to bond well to various types of TE material such as $Bi_2Te_{2.55}Se_{0.45}$,[12] Zn_4Sb_3,[13] (Pb,Sn)Te,[14] and $AgSbTe_{2.01}$.[15] For Mg_2Si-based materials, both Ni and Cu were reported to exhibit good adhesion performance and low contact resistance in bonding experiments using different electrode materials.[16–18]

In practice, an effective TE joint should retain stable microstructure, with low thermal and electrical contact resistance, together with sufficient bonding strength during its long service life. Thus, studying the thermal reliability and mechanical properties of TE joints is necessary. Some investigations on the thermal stability of Ni/Mg_2Si contacts have been conducted in recent years. De Boor et al.[19,20] fabricated Mg_2Si samples with Ni electrodes by using the one-step spark plasma sintering (SPS) method and showed that the Mg_2Si/Ni joints retained low electrical resistance and stable microstructure after annealing at 823 K for 168 h. Zhang et al.[16] reported that the specific contact resistance of the Mg_2Si/Ni interface changed from $10^{-4}\ \Omega\ cm^2$ for the as-grown sample to approximately $10^{-2}\ \Omega\ cm^2$ for the sample annealed at 400°C for 24 h. Sakamoto et al.[21] discovered that the Mg_2Si/TiN/Ni interface exhibited weak long-term adhesion after thermal treatment at 873 K for 1 h. However, we have not found any research on the long-term stability of the Mg_2Si/Cu interface.

In this work, Mg_2Si/Cu samples were prepared using the SPS method. To investigate the high-temperature reliability of the Mg_2Si/Cu contact, the fabricated samples were annealed in vacuum at temperatures of 500°C, 550°C, and 580°C for duration of 24 h, 48 h, and 72 h. The microstructure evolution and the elemental composition of the intermediate layer, along with the contact resistance and shear strength variation of the samples after thermal reliability testing, were investigated. The results showed that the Mg_2Si/Cu joint exhibited good stability during thermal reliability testing at temperature of 500°C for up to 72 h.

EXPERIMENTAL PROCEDURES

Materials

Commercial polycrystalline undoped Mg_2Si powder with purity of 99.5% supplied by Alfa Aesar and Cu powder were used as starting materials. Cu was chosen as electrode material due to its high electrical conductivity (5.9×10^7 S/m), high thermal conductivity (401 W/m/K), and CTE closest to that of Mg_2Si (Fig. 1). The CTE data presented in Fig. 1 were measured by thermal dilatometer (DIL 402C, Netzsch, Germany), being basically in agreement with values listed in Refs. 17 and 22. In our experiment, Cu was directly bonded to Mg_2Si in accordance with the study of Ferrario,[18] where adding an Al or Ti interlayer between Cu and Mg_2Si made the mechanical and contact properties of the interface worse compared with the Cu/Mg_2Si joint.

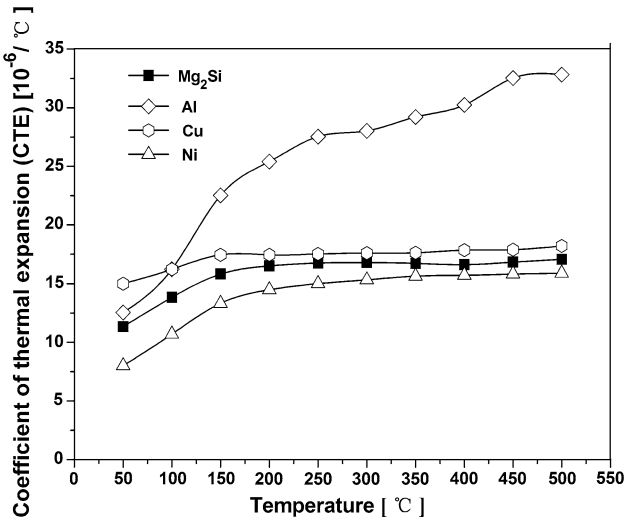

Fig. 1. Measured CTE of commonly used electrode materials (Cu, Ni, Al) and Mg_2Si.

Fabrication of Samples

Mg_2Si/Cu samples were fabricated by SPS method after cold-pressing. The complete experimental procedure is illustrated in Fig. 2. First, pure Cu powder was packed into a steel die (inner diameter 16 mm) and cold-pressed into a foil under pressure of 20 MPa for 10 min using a tablet press (PC-15S, Tianjin Pinchuang Technology Development Co., Ltd.). To avoid nonuniform thickness and poor contact, the obtained Cu foil was polished by using SiC sandpaper with grits of 800, 1000, and 2000 then cleaned using anhydrous ethanol in an ultrasonic cleaner (KQ-100E, Kun Shan Ultrasonic Instruments Co., Ltd.). Second, the prepared Cu foil and Mg_2Si powder were put into a graphite die (inner diameter 16 mm) and compacted using the upper punch. Finally, the graphite die loaded with Mg_2Si powder and Cu foil was sintered by SPS (Dr. Sinter SPS-1050, Sumitomo Coal Mining Co., Ltd., Tokyo, Japan) in vacuum. The optimized sintering parameters—pressure of 50 MPa, temperature of 650°C, and holding time of 10 min—were similar to those reported by Tohei.[23] A series of Mg_2Si/Cu samples were obtained by using the introduced fabrication procedure.

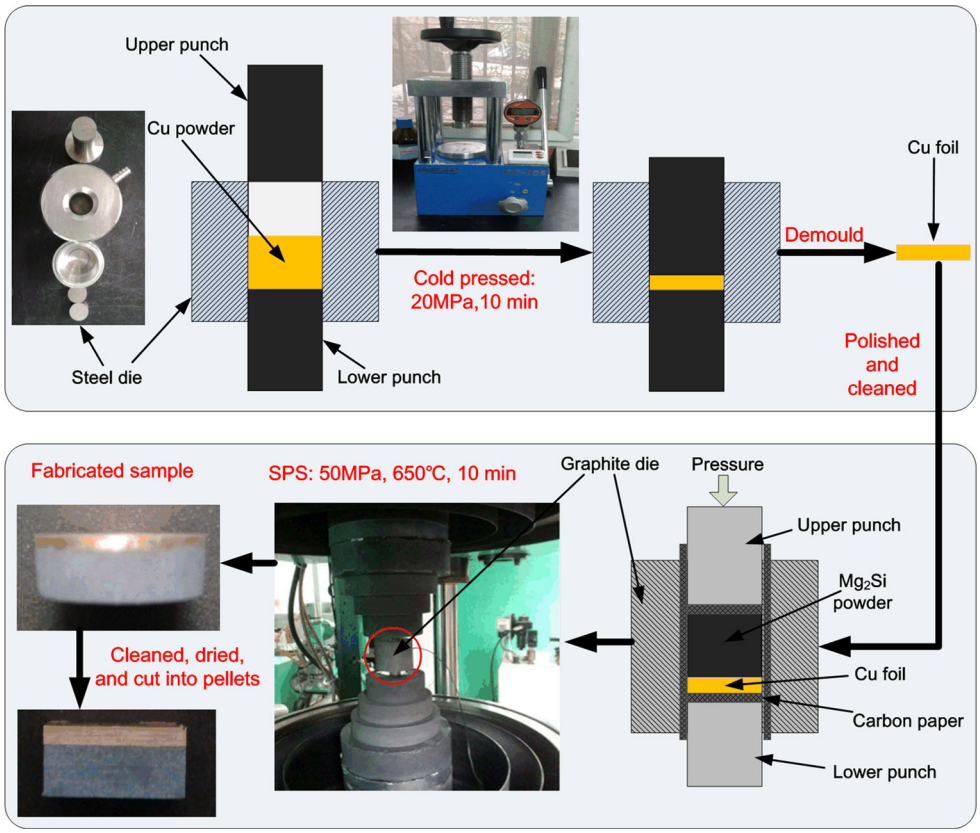

Fig. 2. Experimental procedure for fabrication of Mg_2Si/Cu samples.

Thermal Stability Test

To study the duration of thermal stability, the samples were ultrasonically cleaned, dried, and placed into quartz tubes encapsulated in a vacuum crucible furnace (VBF-1200X-H8, Hefei Kejing Materials Technology Co., Ltd.) for annealing test. Considering the operating temperature of Mg_2Si-based devices of around 500°C, the aging temperature was set at 500°C, 550°C, and 580°C. The aging duration ranged from 0 h to 72 h. The annealed samples were cut to appropriate sizes for measurement of characteristics using a diamond wire-cutting machine (STX-202A, Shenyang Kejing Auto-instrument Co., Ltd.)

Measurement of Characteristics

The microstructure of the interface was observed by scanning electron microscopy (SEM, JSM-5610LV; JEOL). The elemental distribution and chemical composition of the intermediate layer were analyzed by electron probe microanalysis (EPMA, JXA-8230; JEOL). Contact resistance was tested using an in-house-fabricated four-probe apparatus, whose measurement principle is the same as described in Ref. 24. The dimensions of the specimen used for contact resistance measurements were 3.7 mm × 3.7 mm × 7 mm. Shearing tests were carried out using a universal tester (Zwich/Roell, Germany) at low loading speed of 0.5 mm/min. To ensure the accuracy of the experimental results, each of the above measurements was conducted on three specimens.

RESULTS AND DISCUSSION

Microstructure Evolution of Mg_2Si/Cu Joints

The interface microstructure of the three as-grown specimens measured by SEM was similar. Therefore, only one SEM image was selected and is presented in Fig. 3a for analysis, the same treatments being conducted on Fig. 3b–f. As observed in Fig. 3a, a uniform intermediate layer formed between Cu and Mg_2Si during the sintering process, with apparent boundaries among different layers being clearly visible. Furthermore, the interlayer presented good adhesion to both the Mg_2Si and Cu layer. No cracks or defects developed in the samples without thermal treatment, which might be due to the excellent thermal match between Cu and Mg_2Si (Fig. 1). However, one problem that exists with these samples is that the Mg_2Si was not compact enough, as observed in Fig. 3a. The density of Mg_2Si samples sintered at 650°C measured by the Archimedes method was 1.68 g/cm^3, similar to that of $Mg_2Si_{0.9875}Sb_{0.0125}$ reported by De Boor.[25] Compared with the theoretical density of Mg_2Si (about 2.0 g/cm^3), the relative density is only 84%. To make

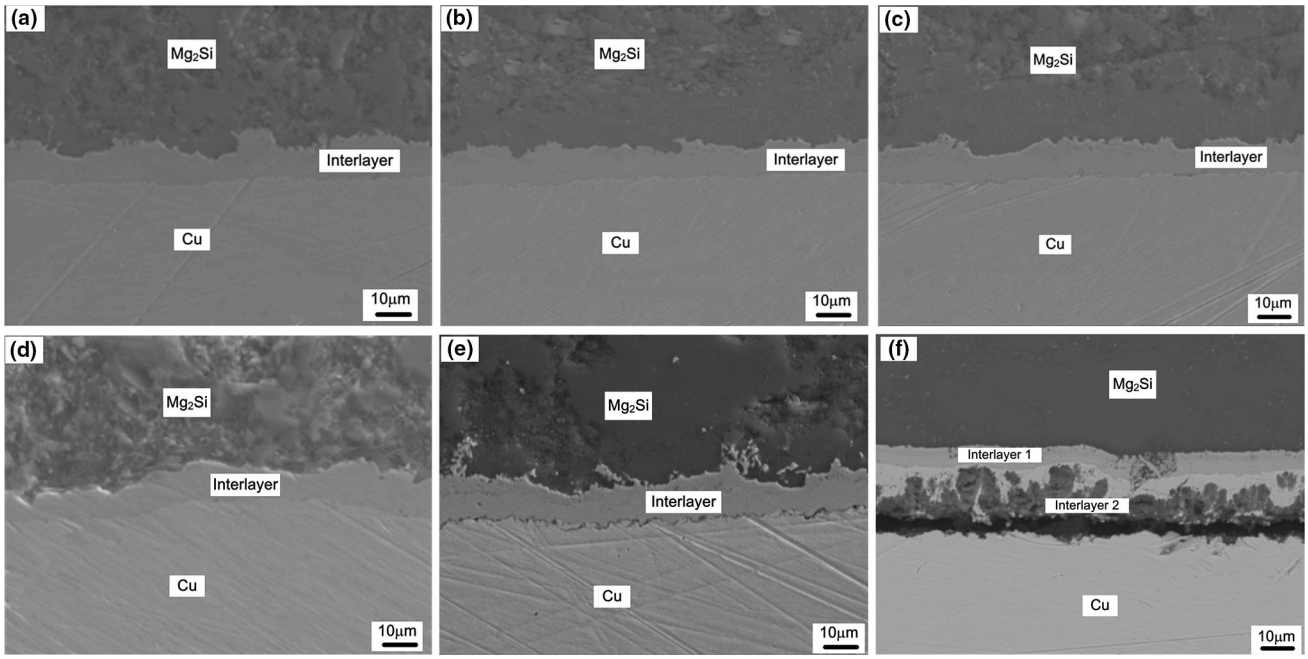

Fig. 3. SEM micrographs of Mg_2Si/Cu junctions: (a) without annealing test, and annealed at (b) 500°C for 24 h, (c) 500°C for 48 h, (d) 500°C for 72 h, (e) 550°C for 24 h, and (f) 580°C for 24 h.

Mg_2Si denser, a higher sintering temperature of 700°C was attempted, but we found that the Cu melted and flowed out. This is presumably because the copper powder is easier to melt due to its small particle size and the high sintering pressure (50 MPa). According to Vivekanandhan's work,[5] relative density of 95% was obtained for pure Mg_2Si sintered at 650°C by using nanostructured Mg-Si powder, which could be used for Mg_2Si/Cu joint fabrication in the future.

To determine the elemental distribution and chemical composition of the interface, EPMA line scan and energy-dispersive x-ray spectroscopy (EDS) point spectrum analysis were carried out. Figure 4a shows the EPMA line scan result of the specimen before thermal treatment. An interlayer composed of Mg, Si, and Cu can be identified from position around 28 μm to 38 μm, indicating thickness of approximately 10 μm. Based on quantitative analysis of point spectrum a1 marked in Fig. 4a, we found that the composition (at.%) of the homogeneous interlayer was Mg:Si:Cu = 36:11:53, as presented in Table I. According to the Mg–Si–Cu phase diagram,[26,27] the third ternary compound τ_3 with approximate chemical formula $(Cu_{0.8}Si_{0.2})_2(Mg_{0.88}Cu_{0.12})$ could exist in solid state at 500°C. The composition range of τ_3 has been reported to be 25 at.% to 35 at.% Mg, 10 at.% to 20 at.% Si, and the rest Cu, in good agreement with the result at a1. Thus, the intermediate phase of the as-sintered samples might correspond to the Mg–Si–Cu ternary mixture τ_3.

To investigate the microstructure evolution behavior during the service life, SEM images of Mg_2Si/Cu joints after annealing at different temperatures for various aging durations are presented in Fig. 3b–f for comparison. It can be seen that Mg_2Si and Cu remained well connected and showed no cracks after annealing at temperature of 500°C for 24 h, 48 h, and 72 h (Fig. 3b–d). However, when the aging temperature was increased to 550°C, a crack extended along the interlayer close to the Cu layer for the Mg_2Si/Cu joint annealed for only 24 h (Fig. 3e). Furthermore, the Cu electrode appeared to delaminate from the Mg_2Si section when the annealing temperature was increased to 580°C (Fig. 3f). The reasons for the crack formation will be expounded in the following paragraph.

Comparing Fig. 4a–e reveals that the thickness of the interlayer exhibited no obvious change when annealed at 500°C or 550°C. The variation in the thickness of the interlayer with annealing conditions is illustrated in Fig. 4f. The small difference (from 10 μm to 12 μm) might be due to the slightly uneven boundary of the intermediate layer and the spatial resolution of the test instruments. Through comparison of the point analysis results of a1 to e1 marked in Fig. 4a–e (Table I), we found that the composition (at.%) of Mg, Si, and Cu in the interlayer remained essentially stable, corresponding to τ_3 phase. In summary, we found that both the thickness and composition of the intermediate layer remained stable after thermal treatment at 500°C for up to 72 h or 550°C for 24 h. However, a phenomenon to be noticed is that cracks occurred in the samples aged at 550°C, probably resulting from release of residual thermal stress caused by the CTE difference between

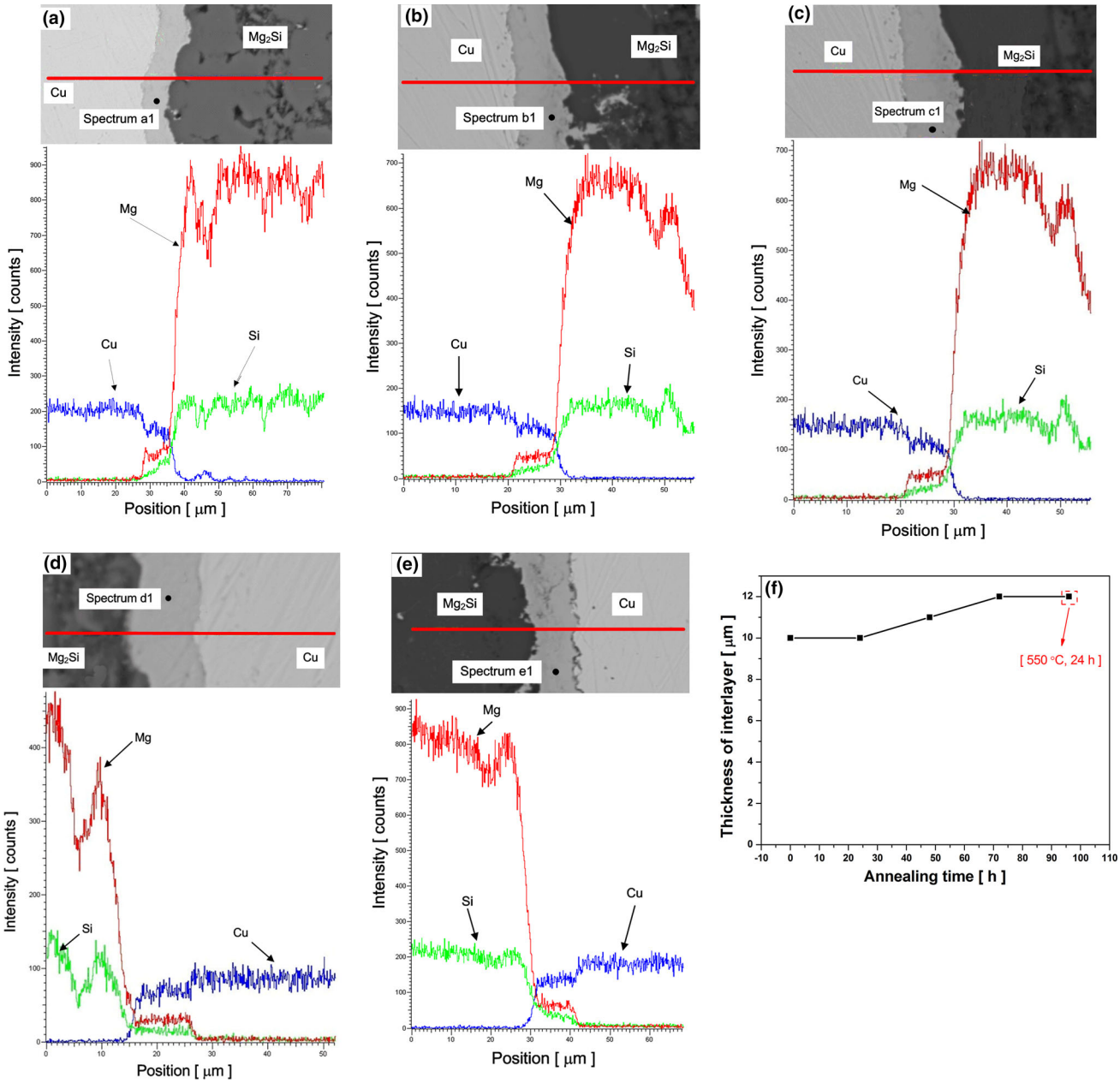

Fig. 4. EPMA line scan results of Mg_2Si/Cu joints annealed at (a) 500°C for 0 h, (b) 500°C for 24 h, (c) 500°C for 48 h, (d) 500°C for 72 h, and (e) 550°C for 24 h, and (f) interlayer thickness versus annealing time (the points marked in the figure were used for EDS point spectrum analysis).

the Cu electrode and τ_3 phase with aging temperature up to 550°C.

The interface microstructure of the specimens annealed at 580°C appeared complicated. As shown in Fig. 3f, a multiphase reaction layer formed between Mg_2Si and Cu: interlayer 1 appeared to be uniform and have a clear boundary, but interlayer 2 was inhomogeneous. Considering the nonuniform and extremely uneven boundary of interlayer 2, EPMA line scanning was not carried out, but point spectrum analysis was conducted on different layers of the interface (Table II). The analysis results at f1 and f2 indicate that the composition of interlayer 1 was essentially in agreement with the as-sintered samples, but the thickness decreased to about 5 μm (Fig. 3f). Therefore, we assumed that the τ_3 phase might become thermodynamically less stable at high temperature of 580°C. A part of the τ_3 decomposed, and further interdiffusion of Mg, Si, and Cu continued. Then, a new reaction layer consisting of binary phase Mg_2Cu (spectrum f4) and an unknown Cu–Mg–Si ternary phase (spectrum f3) developed between τ_3 and the Cu electrode. Considering that the fracture appeared between interlayer 2 and Cu (spectra f5 and f6) rather than inside the Mg_2Cu, we speculate

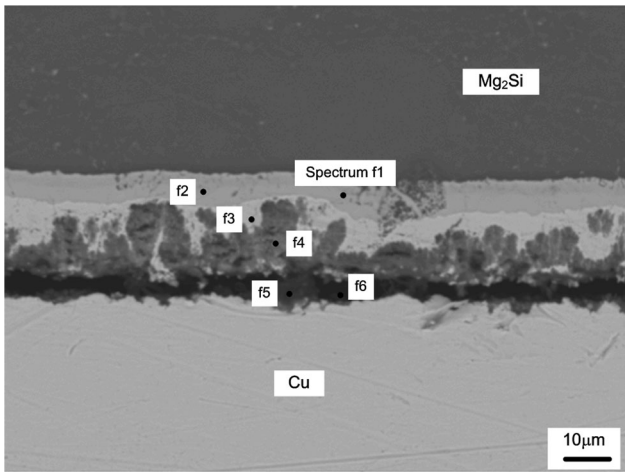

Fig. 5. Backscattering image of Mg_2Si/Cu joint annealed at 580°C for 24 h.

that a possible reason may be the CTE mismatch between Cu and Mg_2Cu.

In summary, to obtain a long lifetime for Mg_2Si/Cu joints, the hot-side operation temperature should not exceed 500°C. The following analyses were conducted only with the specimens annealed at 500°C.

Contact Resistance of Mg_2Si/Cu Junctions

The electrical contact resistance was obtained using a four-probe measurement device with spatial resolution of 10 μm. A schematic of the measurement principle is shown in Fig. 6. A constant current I was applied at the two ends of the tested Mg_2Si/Cu specimen through two fixed probes. The other two probes were located on the surface of the Mg_2Si/Cu sample, one fixed on the surface of the Cu section (set as $x = 0$), while the other could move along the TE leg direction. The electrical potential U between the two probes was measured using a voltmeter inserted between them. Thus, the resistance R of the section between the fixed and mobile probe can be determined as $\frac{U}{I}$. A curve of R versus the location along the TE leg x (R versus x) is thus obtained as the mobile probe reaches different positions. The location of the abrupt change in R is taken as the interface position, and the electrical contact resistance is calculated from the difference of the resistance in the Cu and Mg_2Si sections extrapolated to the junction location.

The measured result of R versus x for the Mg_2Si/Cu specimen before thermal treatment is also shown in Fig. 6. The initial step length for the mobile probe was set as 50 μm. It can be observed that the resistance was nearly zero at the location of the Cu section, which can be attributed to the low electrical resistivity of Cu. From $x = 0.2$ mm to $x = 0.25$ mm, the resistance changed rapidly from nearly zero to 0.13 Ω, which was caused by the contact resistance. As the thickness of the interlayer

Table I. Comparison of interlayer composition with various annealing conditions (points marked in Figs. 4 and 5)

Point Number	Cu (at.%)	Mg (at.%)	Si (at.%)
Spectrum a1	53	36	11
Spectrum b1	53	33	14
Spectrum c1	57	31	12
Spectrum d1	51	38	11
Spectrum e1	55	33	12
Spectrum f1	53	31	16

Table II. Results of point spectrum analysis at six points marked in Fig. 5

Point Number	Cu (at.%)	Mg (at.%)	Si (at.%)
Spectrum f1	53	31	16
Spectrum f2	55	31	14
Spectrum f3	75	9	16
Spectrum f4	31	65	4
Spectrum f5	86	9	5
Spectrum f6	98	2	0

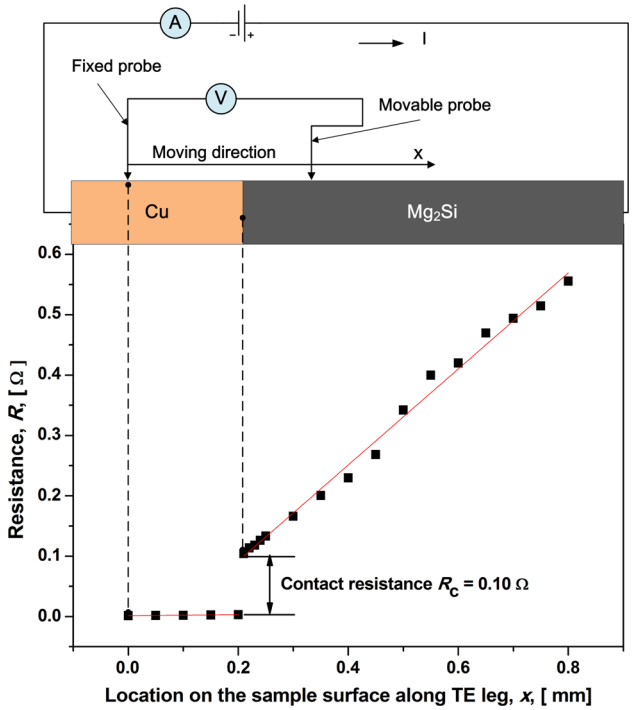

Fig. 6. Schematic of electrical contact resistance measurement principle together with tested resistance varying with location x along the TE leg for as-grown Mg_2Si/Cu joint.

was approximately 10 μm, as described in "Microstructure Evolution of Mg_2Si/Cu Joints" section, the interface position should be determined more accurately. Thus, a smaller step length of 10 μm

was utilized to measure the resistance from $x = 0.25$ mm back to $x = 0.2$ mm to obtain much denser data. Further test results showed that the location $x = 0.21$ mm could be the interface position between Mg_2Si and Cu, and the calculated electrical contact resistance R_c was approximately 0.10 Ω. The specific contact resistance r_c can be calculated as $r_c = R_c \times A$, where A is the cross-sectional area of the measured specimen. The calculated r_c was 13.7 mΩ cm^2, comparable to the value of 8.1×10^{-3} Ω cm^2 of sample S3 (undoped Mg_2Si)/Cu + TT presented in Ferrario's work.[18] The slight difference may be due to the different fabrication methods applied. However, a large difference exists between the measured contact resistance in this work and the lowest value obtained for doped Mg_2Si by Ferrario. This can be attributed to the fact that the specific contact resistance decreases with increasing carrier concentration of the TE material through the doping technique. Thus, the value of r_c may decrease if doped Mg_2Si materials are used in the experiment.

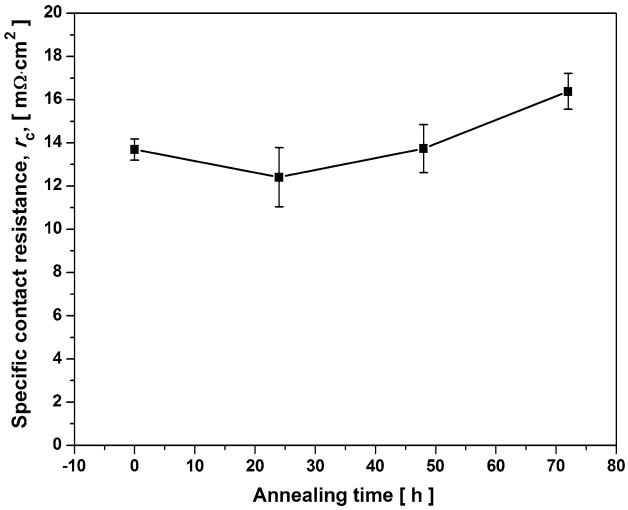

Fig. 7. Variation of specific contact resistance of Mg_2Si/Cu joints with aging time (at temperature of 500°C).

The specific contact resistance of other specimens after thermal treatment at 500°C for different aging durations was obtained using the same method, as shown in Fig. 7. It can be observed that the specific contact resistance decreased slightly for the Mg_2Si/Cu joint annealed for 24 h, then increased slightly with increasing aging time up to 72 h. The reason might be that the thickness and composition of the interface layer between Mg_2Si and Cu did not change significantly due to the thermal treatment at 500°C. The Mg_2Si/Cu contacts retained relatively stable specific contact resistance lower than 16.4 mΩ cm^2 after annealing at temperature of 500°C for 72 h.

Mechanical Properties of Mg_2Si/Cu Joints

For practical applications, the interface between the TE element and electrode must be strong enough that the joint does not break during service. Thus, shear tests were conducted on Mg_2Si/Cu samples. Figure 8 shows the tested specimen and a schematic view of the shear test. The specimen used for shear testing was first cut into the shape shown in Fig. 8a, then held using the clamp apparatus in the shear tester. The loading force F was applied to the Cu section close to the interface until the joint broke. The shear strength was then obtained by dividing the breaking load by the contact area of 3.8 mm × 2.6 mm.

Figure 9a shows the measured shear strength of Mg_2Si/Cu joints annealed at 500°C for various aging durations from 0 h to 72 h. The shear strength decreased with increasing annealing time. The greatest strength of 16.2 MPa was obtained for the Mg_2Si/Cu sample without annealing, similar to that of case no. 3 reported in Ref. 23. After annealing for 24 h, the shear strength decreased to 15.1 MPa, and it further declined to 12.8 MPa and 10.7 MPa with prolonged aging time to 48 h and 72 h, respectively. The shear strength of the sample after 72 h of thermal

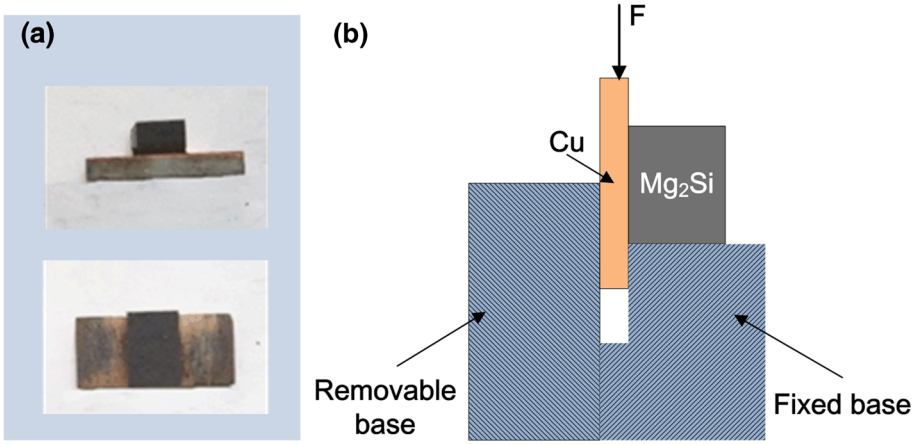

Fig. 8. Shear test: (a) Mg_2Si/Cu samples used for the shear test; (b) schematic view of shear test.

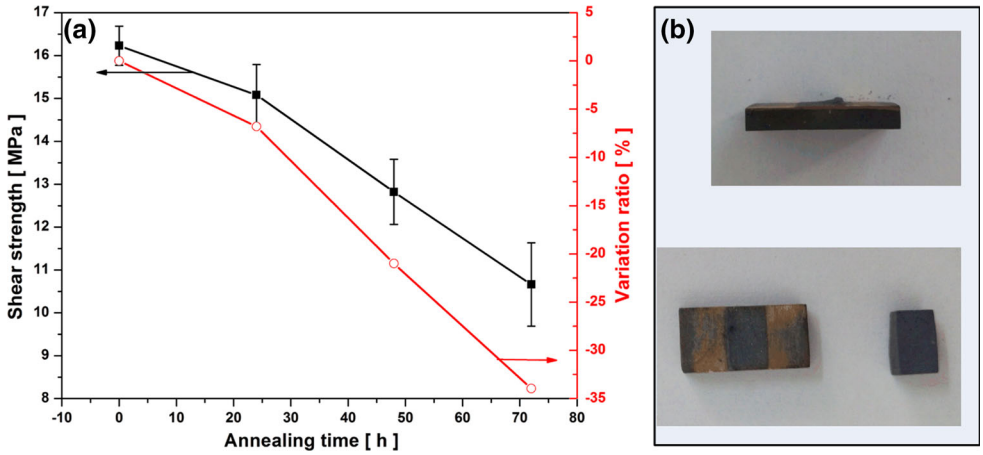

Fig. 9. Shear test results: (a) variation of shear strength of Mg_2Si/Cu joints with aging duration (at temperature of 500°C); (b) fracture surface of Mg_2Si/Cu samples after shear test.

treatment decreased by 34% compared with the samples without annealing. To analyze the factors causing this decline in the shear strength of the joints, we examined the fracture surface of the tested specimens. As shown in Fig. 9b, the breakage of all the tested specimens did not really occur at the interface but within the interior of the Mg_2Si section, close to the interface. Similar fracture developed in case no. 3 reported by Tohei.[23] The change in shear stress with annealing time is not due to degradation of the interface but to the material properties themselves. The well-known Hall–Petch equation implies that the strength of the polycrystal increases as the grain size decreases. Previous studies by Itoh[28] and Wang[29] indicated that the grain size of Mg_2Si increases with increasing aging time. Thus, we can deduce that the shear strength of Mg_2Si decreased as the annealing time increased, which explains why the bonding strength of the joint declined with increasing aging time. To improve the bonding strength of the joints further, one could enhance the mechanical properties of Mg_2Si materials through grain refinement using nanostructuring and element doping strategies[30] in the future.

CONCLUSIONS

A series of Mg_2Si/Cu samples were fabricated using the SPS method. The thermal stability of the fabricated joints was investigated by annealing testing at temperatures of 500°C, 550°C, and 580°C for various durations up to 72 h. Through sintering, Mg_2Si/Cu junctions were bonded well due to production of a reaction layer consisting of ternary phase τ_3 with approximate composition $(Cu_{0.8}Si_{0.2})_2(Mg_{0.88}Cu_{0.12})$. The measured specific contact resistance and shear strength were 13.7 mΩ cm^2 and 16.2 MPa for the as-grown junctions. After thermal treatment at 500°C for 72 h, the thickness and composition of the intermediate layer exhibited no obvious change, resulting in stable electrical contact resistance. The shear strength decreased by 34%, due to degradation of the substrate material rather than the interface itself. However, cracks developed along the interlayer close to the Cu layer when the aging temperature was increased to 550°C or 580°C. These results show that the Mg_2Si/Cu joints possessed high-temperature reliability with stable microstructure and electrical contact, as well as sufficient bonding strength when operating at 500°C. Further study on improvement in the interface performance could be carried out by using doped or nanostructured Mg_2Si materials.

ACKNOWLEDGEMENTS

This work was financially supported by the National Natural Science Foundation of China (No. 51272198), International S&T Cooperation Program of China (2014DFA63070), Program for the Commercialization of Research Findings of Qinghai (2016-GX-118), National High-Tech R&D Program of China (863 Program, No. 2012AA051104), and Fundamental Research Funds for the Central Universities (WUT, Nos. 2016-III-009 and 2017-III-002).

REFERENCES

1. X.F. Zheng, C.X. Liu, Y.Y. Yan, and Q. Wang, *Renew. Sustain. Energy Rev.* 32, 486 (2014).
2. P. Gao, I. Berkun, R.D. Schmidt, M.F. Luzenski, X. Lu, P.B. Sarac, E.D. Case, and T.P. Hogan, *J. Electron. Mater.* 43, 1790 (2014).
3. A.U. Khan, N.V. Vlachos, E. Hatzikraniotis, G.S. Polymeris, C.B. Lioutas, E.C. Stefanaki, K.M. Paraskevopoulos, I. Giapintzakis, and T. Kyratsi, *Acta Mater.* 77, 43 (2014).
4. N. Vlachos, G.S. Polymeris, M. Manoli, E. Hatzikraniotis, A.U. Khan, C.B. Lioutas, E.C. Stefanaki, E. Pavlidou, K.M. Paraskevopoulos, J. Giapintzakis, and T. Kyratsi, *J. Alloys Compd.* 714, 502 (2017).
5. P. Vivekanandhan, R. Murugasami, V.R.S. Sairam Kalahasti, and S. Kumaran, *Powder Technol.* 319, 129 (2017).
6. Q. Zhang, Y. Zheng, X. Su, K. Yin, X. Tang, and C. Uher, *Scr. Mater.* 96, 1 (2015).

7. A.T. Burkov, P.P. Konstantinov, M.I. Fedorov, M. Manoli, T. Kyratsi, K. Tarantik, and M. Jaegle, *Mater. Today: Proc.* 2, 596 (2015).
8. K. Yin, Q. Zhang, Y. Zheng, X. Su, X. Tang, and C. Uher, *J. Mater. Chem. C* 3, 10381 (2015).
9. H. Xia, F. Drymiotis, C. Chen, A. Wu, and G.J. Snyder, *J. Mater. Sci.* 49, 1716 (2014).
10. X.C. Fan, M. Gu, X. Shi, L.D. Chen, S.Q. Bai, and R. Nunna, *Ceram. Int.* 41, 7590 (2015).
11. L. Shi, X. Huang, M. Gu, and L. Chen, *Surf. Coat. Technol.* 285, 312 (2016).
12. C.-H. Chuang, Y.-C. Lin, and C.-W. Lin, *Metals* 6, 92 (2016). https://doi.org/10.3390/met6040092.
13. Y.C. Lin, K.T. Lee, J.D. Hwang, H.S. Chu, C.C. Hsu, S.C. Chen, and T.H. Chuang, *J. Electron. Mater.* 45, 4935 (2016).
14. T.H. Chuang, H.J. Lin, C.H. Chuang, W.T. Yeh, J.D. Hwang, and H.S. Chu, *J. Electron. Mater.* 43, 4610 (2014).
15. H. Li, H. Jing, Y. Han, G. Lu, L. Xu, and T. Liu, *Mater. Des.* 89, 604 (2016).
16. B. Zhang, T. Zheng, Q. Wang, Y. Zhu, H.N. Alshareef, M.J. Kim, and B.E. Gnade, *J. Alloys Compd.* 699, 1134 (2017).
17. P. Gao, *Mg_2(Si,Sn)-Based Thermoelectric Materials and Devices* (Michigan State University, Ann Arbor, 2016), p. 139.
18. A. Ferrario, S. Battiston, S. Boldrini, T. Sakamoto, E. Miorin, A. Famengo, A. Miozzo, S. Fiameni, T. Iida, and M. Fabrizio, *Mater. Today: Proc.* 2, 573 (2015).
19. J. de Boor, C. Gloanec, H. Kolb, R. Sottong, P. Ziolkowski, and E. Mueller, *J. Alloys Compd.* 632, 348 (2015).
20. J. De Boor, D. Droste, C. Schneider, J. Janek, and E. Mueller, *J. Electron. Mater.* 45, 5313 (2016).
21. T. Sakamoto, Y. Taguchi, T. Kutsuwa, K. Ichimi, and S. Kasatani, *J. Electron. Mater.* 45, 1321 (2016).
22. G. Chen, T. Liu, X. Tang, X. Su, and Y. Yan, *J. Inorg. Mater.* 30, 639 (2015).
23. T. Tohei, S. Fujiwara, T. Jinushi, and Z. Ishijima, *IOP Conf. Ser. Mater. Sci. Eng.* 61, 12035 (2014).
24. Y. Thimont, Q. Lognone, C. Goupil, F. Gascoin, and E. Guilmeau, *J. Electron. Mater.* 43, 2023 (2014).
25. J. de Boor, C. Compere, T. Dasgupta, C. Stiewe, H. Kolb, A. Schmitz, and E. Mueller, *J. Mater. Sci.* 49, 3196 (2014).
26. P. Perrot, in *Light Metal Systems. Part 4: Selected Systems from Al-Si-Ti to Ni-Si-Ti*, ed. by G. Effenberg and S. Ilyenko (Springer, Berlin, 2006), p. 1-14.
27. J. Zhao, J. Zhou, S. Liu, Y. Du, S. Tang, and Y. Yang, *J. Min. Metall. B* 52, 99 (2016).
28. T. Itoh and A. Tominaga, *Mater. Trans.* 57, 1088 (2016).
29. L. Wang, X.Y. Qin, W. Xiong, L. Chen, and M.G. Kong, *Mater. Sci. Eng. A Struct.* 434, 166 (2006).
30. Q.S. Meng, W.H. Fan, R.X. Chen, and Z.A. Munir, *J. Alloys Compd.* 509, 7922 (2011).